Analysis of Curved Optical Waveguides by Conformal Transformation

MORDEHAI HEIBLUM, STUDENT MEMBER, IEEE, AND JAY H. HARRIS, MEMBER, IEEE

Abstract—The method of conformal transformations is applied to the analysis of waveguide bends. Equivalent structures are obtained that permit solution by traditional methods of optical waveguide analysis. Losses associated with both curvature and with the transition from straight to curved guides are discussed and simple first-order expressions that describe the dependence of the losses on waveguide parameters are derived.

I. INTRODUCTION

CONFORMAL transformations provide a method for analyzing curved or otherwise varying waveguides that not only yields useful data concerning wave configurations and attenuation rates but also generates an equivalent structure whose properties may be readily appreciated on an intuitive level. Primary interest in this paper is centered on bend losses in curved waveguides. This determination is central to the design of integrated optical systems because switches and arrays of switches utilizing cylindrical waveguides require geometric displacements that are provided by bends.

The bend-loss problem has been previously investigated by Marcatili, Marcuse, and Lewin [1-a)–1-c)] using the established [2] technique of representing the field in the external region by a cylinder (Hankel) function of complex order and matching to fields in the guide that are assumed unperturbed from a straight guide. The transformations result in an analysis that differs from this previous work in that guides with a continuously varying refractive index such as diffused guides may be treated, in that radii of curvature need not be restricted to large values, and in that losses associated with a change in the direction of curvature required for a bend can be treated. Taylor [3] has also treated the bend problem using a computer-based analysis. Transformations not only provide an analytic approach but also avoid certain assumptions necessary for the efficient application of numerical methods.

Conformal transformations apply to solutions of the two-dimensional scalar wave equation

$$[\nabla^2_{x,y} + k^2(x,y)]\psi = 0. \tag{1}$$

Solutions are obtained in a coordinate system u, v defined with respect to x and y by the relation

$$W = u + iv = f(Z) = f(x + iy) \tag{2}$$

where f is an analytic function. Expanding $\nabla^2_{x,y}$ in (1) with the aid of the Cauchy Riemann relations ($\partial u/\partial x = \partial v/\partial y$, $\partial u/\partial y = -\partial v/\partial x$), (1) may be expressed as

$$\left[\nabla^2_{u,v} + \left|\frac{dZ}{dW}\right|^2 k^2(x(u,v), y(u,v))\right]\psi = 0 \tag{3}$$

where $|dW/dZ|^2 = (\partial u/\partial x)^2 + (\partial v/\partial x)^2$. Equation (3) is a well-known relation [4]. The objective of the transformation is to select an $f(Z)$ that converts curved boundaries in the x, y plane to straight ones in the u, v plane. Before discussing this matter further (see Section II) we wish to enumerate the kinds of integrated optical problems to which solutions to (1) are applicable.

1) TE mode on a planar guide. The guide is uniform in z with discrete or continuous index variation in x and y. The fields are constant in z and E has only a z component which we identify as ψ, i.e., $E = \psi(x, y)\hat{z}$. Boundary conditions require continuity of ψ and $\nabla\psi$ and this continuity is maintained in the x, y plane if it is imposed in the u, v plane.

2) TM mode on a planar guide with discrete index variations and $H = \psi(x, y)\hat{z}$. ψ is continuous and $(1/\epsilon)\nabla\psi$ is continuous.

3) TM mode on a planar guide with continuous index variation. In this case the wave equation for H_z is

$$[\nabla^2_{x,y} + (\nabla_{x,y}\epsilon/\epsilon) \cdot \nabla_{x,y} + k^2(x,y)]H_z = 0 \tag{4}$$

and in the u, v coordinate system

$$[\nabla^2_{u,v} + (\nabla_{u,v}\epsilon/\epsilon) \cdot \nabla_{u,v} + \left|\frac{dZ}{dW}\right|^2 k^2(x(u,v), y(u,v))]\psi = 0. \tag{5}$$

Although we concentrate on solutions to (1), the method of analysis is applicable to (4) or (5) as will be indicated.

4) Approximately applicable to cylindrical[1] waveguides that are uniform in the z direction. An example is a diffused waveguide [5] of rectangular cross section that undergoes a bend in the x, y plane. Using potential functions $A^{\text{TE}}(x, y, z)\hat{z}$ and $A^{\text{TM}}(x, y, z)\hat{z}$ that yield TE to z fields with $E = \nabla \times A^{\text{TE}}\hat{z}$ and TM to z fields with $H = \nabla \times A^{\text{TM}}\hat{z}$, approximate solutions to the wave equation can be expressed

$$A^{\text{TM}}(x, y, z) = g^{\text{TM}}(z)\psi(x, y). \tag{6}$$

For a guide centered about $y = 0$ and $z = 0$, $g(z)$ is a solution of

$$\left[\frac{\partial^2}{\partial z^2} + k^2(0, 0, z)\right]g(z) = k^2_w g(z) \tag{7}$$

where k_w is the wave-propagation constant for a planar guide. ψ is a solution of

M. Heiblum is with the Department of Electrical Engineering and Computer Sciences, University of California, Berkeley, Calif.
J. H. Harris is with the National Science Foundation, Washington, D.C.

[1] Also referred to as linear, two-dimensionally confined, and three-dimensional waveguides.

$$[\nabla^2_{x,y} + k^2(x, y, 0) - (k^2(0, 0, 0) - k^2_w)] \psi = 0. \qquad (8)$$

We may identify (8) with (1) using a $k^2(x, y)$ in (1) that is modified by a constant. An equation of the form (5) results for A^{TE}. It is not our purpose to consider the approximation (6)–(8) in detail. This is a complex problem that has received only limited attention [6]. We wish merely to point out that within a customary approximation that derives from the field behavior in a rectangular waveguide with perfectly conducting walls, (1) may be employed to estimate the wave function in curved versions of such important integrated optical structures as diffused guides.

II. EQUIVALENT WAVEGUIDE STRUCTURES

To illustrate the intuitive approach that conformal transformations provide, consider Fig. 1(a), which shows a circularly curved dielectric waveguide with a step discontinuity in refractive index at radii R_1 and R_2. Wave propagation along this structure is described by (1) in which $k^2(x, y)$ appears as a constant in each of the regions of the structure. Using the conformal transformation

$$W = R_2 \ln Z/R_2 \qquad (9)$$

for which

$$\left| \frac{dZ}{dW} \right| = \exp(u/R_2) \qquad (10)$$

(3) is found to describe the waveguide shown in Fig. 1(b). In the W plane the walls are straight and lie between $u = 0$ and $u = -R_2 \ln R_2/R_1$. The refractive index in the structure is the product of (10) and the refractive index in the appropriate region of the curved guide. Those familiar with optical waveguides will note that the index profile of the equivalent structure resembles that in a prism coupler [9]. It is clear that all of the modes of the equivalent structure will radiate to the right where the refractive index exceeds the maximum refractive index in the guide.

If the waveguide in Fig. 1 were a diffused guide in a substrate, as an important practical example, the process of lateral diffusion would result in an index profile of the kind illustrated in Fig. 2(a). The modes on the equivalent guide in Fig. 2(b) are radiative as before. Furthermore, unless the decay rate $n_3(\rho)$ of the lateral diffusion is sufficiently rapid the minimum on the right side of the curve in Fig. 2(b) will cease to appear and there will be no confined modes. This "critical decay" condition is readily found by setting $n_3(\rho) = |dZ/dW|^{-1}$ and results in the requirement

$$n_3(\rho) < n_2 \cdot (R_2/\rho) \qquad R_2 < \rho < (n_2/n_1)R_2. \qquad (11)$$

When the equality of (11) is met, the right side of Fig. 2(b) is constant at value n_2 in the manner depicted in Fig. 3. If there are no guided waves in the equivalent structure, neither will there be any in the curved waveguide.

The circular structure with one boundary illustrated in Fig. 4 will also support guided, albeit lossy waves [12]. This is made apparent by the equivalent guide of Fig. 4(b). We have $n_2 < n_1$ in this case. The guided waves on this structure will have wave refractive indices n_w that lie in the range $n_1 > n_w >$
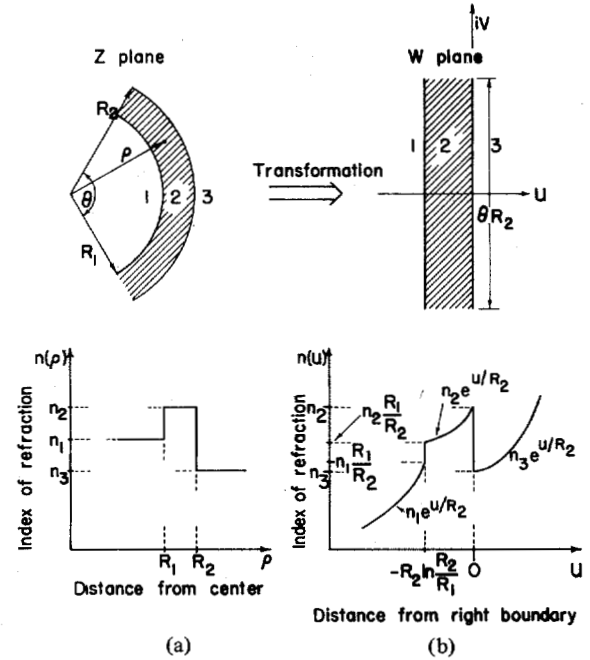

Fig. 1. A two-dimensional bend with step index distribution (a) and its transformation (b).
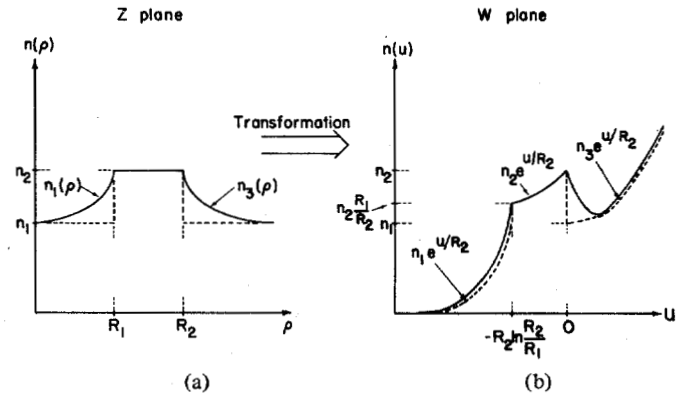

Fig. 2. Index distribution of a diffused bend (a) and its transformation (b). (Dashed lines denote the transformed step distribution bend.)
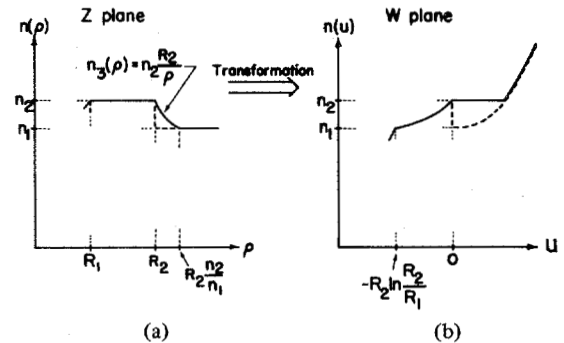

Fig. 3. Index distribution of a diffused guide at "critical decay" for which waveguiding ceases.

n_2 and the waves themselves will be confined to the range $0 > u > R \ln n_2/n_1$. The latter limit is indicated in Fig. 5(a) as u_0. In the original structure this boundary appears at $\rho_0 = R \cdot (n_2/n_1)$. As illustrated in Fig. 5(b), a ray tangent to the circle of radius ρ_0 will strike the tangent to the boundary of
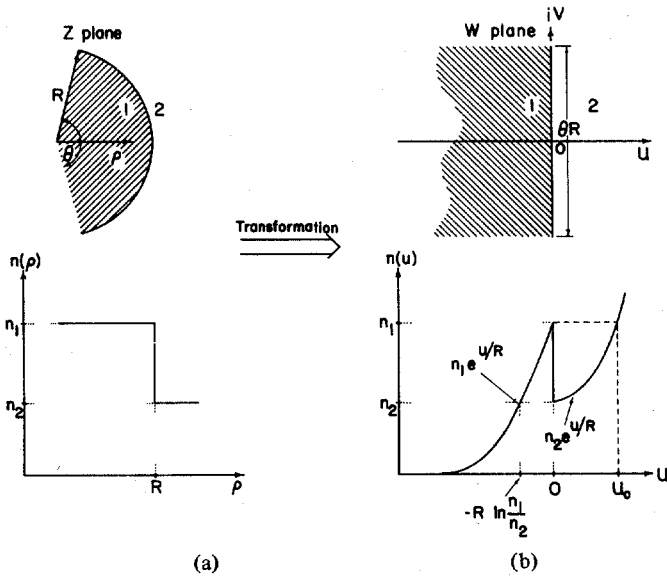
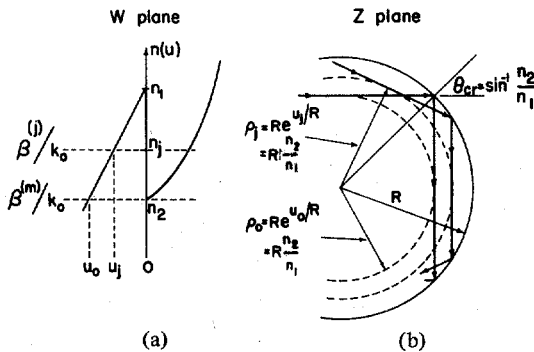Fig. 4. A two-dimensional one-boundary bend with step index distribution (a) and its transformation (b).

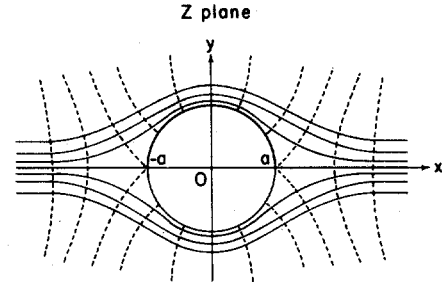Fig. 5. Ray picture of modes j and m that propagate in the guide of Fig. 4.

Fig. 6. Equipotential and streamlines of a conducting cylinder placed in a uniform electric field. The transformation $W = Z + a^2/Z$ converts curved guides whose shape is that of any two streamlines into waveguides with straight boundaries.
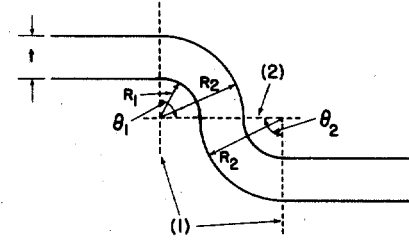

Fig. 7. Waveguide displacement produced by two circular bends. Dotted lines show transition regions.

the circular medium at the critical angle. Rays tangent to circles greater than ρ_0 are (nearly) totally reflected from the boundary while rays tangent to smaller circles are incident at angles less than the critical angle and pass through the boundary.

There are a number of transformations in addition to the logarithmic one (9) that are of potential interest in connection with integrated optics. One class of such transformations may be obtained from familiar equipotential surfaces and streamlines of electrostatics or laminar flow problems. Fig. 6, for example, shows the surfaces obtained when a conducting cylinder is placed in a uniform electric field. The transformation

$$W = Z + \frac{a^2}{Z}$$ (12)

applies to this situation with u equals constant defining the equipotential surfaces, and v equals constant defining the streamlines. If we have an optical waveguide with tapered walls (a horn-shaped structure [7] obtained by flaring a waveguide for coupling purposes, for example) that has the appearance of a segment of any two streamlines in Fig. 6, the transformation (12) will convert the waveguide into one with straight

walls. By varying a in (12), a wide variety of waveguide shapes can be generated. The refractive index in the equivalent structure varies along the guide as well as across it. This situation differs from the transformation (9) where the equivalent structure is uniform in the direction of propagation and necessitates a more complex analysis [8].

The waveguide bend illustrated in Fig. 7 represents an important passive integrated optical component. Under appropriate design the bend can consist of two sections of circular arcs connected to each other and to straight waveguide sections, as indicated by the dotted lines in Fig. 7. The arcs need not be 90° in length as in the figure. Loss mechanisms in this structure include the radiative loss due to modal attenuation along the bends and transition losses that occur between guides at the dotted lines. The remainder of the paper is devoted to an analysis of these effects that is based on the transformation (9).

III. ATTENUATION ALONG A BEND

Strictly speaking, the solution of (3) for structures with refractive index distributions of the kind shown in Figs. 1, 2, and 4 does not contain any guided waves because the refractive index at $u = \infty$ is greater than it is elsewhere. The region to the left of the minimum in refractive index can support a guided wave, however, and from a practical point of view, a field of the form

$$\psi(u, v) = F(u) \exp [i(\beta + i\alpha)v] = F(u) \exp [i(\beta + i\alpha)R_2\theta],$$
$$u < u_6$$ (13)

can be used to represent the guided wave as in the prism coupler [9]. In this expression β and α are the respective propagation and attenuation constants of the wave, θ is the angular and $R_2\theta$ the actual length of the bend along the greater

arc, and $F(u)$ is the spatial characterization of the wave. Equation (13) can be used to the left of the turning point indicated as u_6 in Fig. 8 where $n(u_6) = \beta/k_0$.

$F(u)$, β, and α are functions of the radii of curvature of the bend. Characteristics of $F(u(x, y))$ determine transmission losses as the wave proceeds from one section to the next. This loss is discussed in Section IV. For the present we consider properties of β and α of a uniform bend. For the general structure shown in Fig. 8, β and α may be obtained as the solution of an eigenvalue equation that we express as

$$D_{1,6}(k_v)\big|_{k_v = \beta + i\alpha} = 0. \qquad (14)$$

$D_{1,6}$, termed the "system function" for the structure, is a function of a wavenumber k_v. At certain values of k_v, $D_{1,6}$ is zero and these values are the complex propagation constants for waves on the structure.

The system function is the determinant obtained by matching boundary conditions for a multilayer structure when waves of arbitrary amplitude are assumed to exist in each layer. The system function for step index profiles is discussed in the Appendix. Our interest lies in the system function for continuously varying index profiles which can be obtained in the manner indicated in the Appendix. The method consists of subdividing the structure into thin slabs as indicated in Fig. 8, writing the expression for $D_{1,6}$ for a multilayer, and then taking the limit as the thickness of each slab reduces to differential dimensions. The limit procedure results in a series that must be expressed differently on each side of the turning points u_1, u_4, u_6 of Fig. 8 and in the vicinity of the turning points. The series expressions are presented in [11]. We will obtain approximate expressions by employing the first term of this series expression which involves Wentzel–Kramers–Brillouin (WKB) related approximations shown in the Appendix.

To present the equations to determine β and α we use the symbol k_u to represent the wavenumber

$$k_u(u) = [k_0^2 n^2(u) - k_v^2]^{1/2} \qquad (15)$$

and define integrals over k_u as

$$h_{ij} = \int_{u_i}^{u_j} k_u(u)\, du. \qquad (16)$$

The approximate eigenvalue equation for a wave propagating on the structure lying to the left of u_5 in Fig. 8 is found to be [see (A11)]

$$h_{2,3} + \left(h_{1^+,2} - \tan^{-1}\frac{K_{1^-}}{iK_{1^+}}\right) + \left(h_{3,4^-} - \tan^{-1}\frac{K_{4^+}}{iK_{4^-}}\right) = m\pi$$
$$(17)$$

where

$$K_{j^+,^-} = \begin{cases} k_u\big|_{u_{j^+,-}}, & \text{for solutions of (3)} \\[2ex] \dfrac{k_u}{\epsilon}\Big|_{u_{j^+,-}}, & \text{for solutions of (5).} \end{cases} \qquad (18)$$
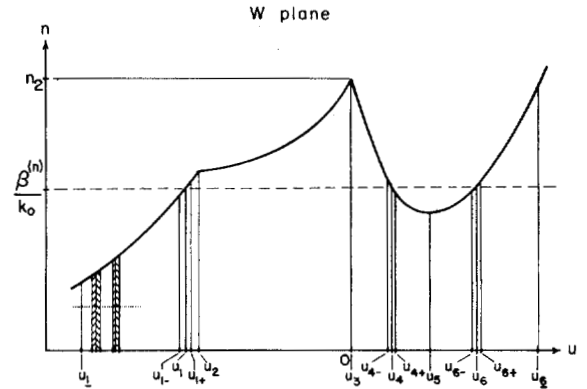

Fig. 8. Transformed index distribution of a bent guide with continuous index distribution. The turning points are u_1, u_4, and u_6. u_{1^+}, u_{1^-}, etc., define the positions at which the representation of the system function changes. The original straight guide has constant index between u_2 and u_3. u_1 and u_6 are arbitrary points beyond u_1 and u_6. To the right of u_1 some sublayers are shown that are used to reduce the system function for discrete layers to the system function of a continuously varying index distribution. (Characters with underbars in the figure appear boldface in text.)

Insight into (17) may be obtained by considering the simple uniform, straight-step index guide. For such a guide $n(u)$ is piecewise constant and the regions $u_{1^+} \to u_2$ and $u_3 \to u_{4^-}$ are of zero length. Equation (17) then reduces to

$$k_u t = m\pi + \tan^{-1}\frac{K_{1^-}}{iK_{1^+}} + \tan^{-1}\frac{K_{4^+}}{iK_{4^-}} \qquad (19)$$

where t is the guide thickness and m is the mode order. This is the familiar eigenvalue equation for waveguides. The terms $\tan^{-1} K_{j^-}/iK_{j^+}$ are functions of k_v and take values between 0 and $\pi/2$ for a step discontinuity. At a continuous turning point, such as appears in Figs. 2 and 8, we may take $\tan^{-1} K_{j^-}/iK_{j^+}$ to be $\pi/4$ based on the assumption that u_{j^+} and u_{j^-} are selected to achieve this result. A more precise specification of the location of these points is discussed in Section IV. We will discuss examples of (17) for index distributions appropriate to waveguide bends following the discussion of α.

Using the same WKB-type approximation as is used to obtain (17), the change in propagation constant due to the presence of the high refractive index region on the right of Figs. 1, 2, 4 may be expressed

$$i\alpha = -\frac{1}{L}\left(\frac{K_{6^+} - K_{6^-}}{K_{6^+} + K_{6^-}}\right)\sin\left(2\tan^{-1}\frac{K_{4^-}}{iK_{4^+}}\right)\exp\left(2ih_{4^+,6^-}\right)$$

$$\simeq \frac{i}{L}\sin\left(2\tan^{-1}\frac{K_{4^-}}{iK_{4^+}}\right)\exp\left(2ih_{4^+,6^-}\right) \qquad (20)$$

as obtained from (A12).

The terms in (20) are to be evaluated at β, the solution of (17). This renders $h_{4^+,6^-}$ positive imaginary in (20) and the exponential in (20), which may achieve small values, largely determines the behavior of α. The parameter L is the derivative of (17), viz.,

$$L = -\frac{\partial}{\partial k_v}\left[h_{2,3} + \left(h_{1^+,2} - \tan^{-1}\frac{K_{1^-}}{iK_{1^+}}\right)\right.$$
$$\left. + \left(h_{3,4^-} - \tan^{-1}\frac{K_{4^+}}{iK_{4^-}}\right)\right]_{k_v = \beta} \qquad (21)$$

and may be termed the *effective longitudinal ray length*. For TE modes in a uniform, straight guide ($h_{1^+,2} = h_{3,4^-} = 0$, $K_{i^\pm} = (k_u)_{u_{i^\pm}}$), for example, L is

$$L = \frac{\beta}{(k_u)_{u_3}}[t + 1/|k_u|_{u_{1^-}} + 1/|k_u|_{u_{4^+}}] = (\tan \phi)[t'] \qquad (22)$$

where t' is the effective width of the waveguide, which includes the decay distances, and ϕ is the angle the wave normal in the guide makes with the surface of the guide (Fig. 9). The second equality in (20) follows from the assumption that u_{6^+} and u_{6^-} are selected so that $K_{6^+} = K_{6^-}/i$. For a continuous change in index at u_4 the sine function in (20) can be approximated by unity.

To further examine the equations for β and α we note that in regions in which the refractive index is constant in x, y, the equivalent index is $n(u) = n \exp u/R$. The resulting expression for $h_{i,j}$ can be integrated in closed form. As an example, for the single-boundary guide of Fig. 4, only $h_{1^+,2}$ of the h's is non-zero in (17). Taking $u_{1^+} = -R \ln (k_0 n_1/\beta)$ and $u_2 = 0$ we find the eigenvalue equation for β of a TE mode (3) to be

$$R\beta\left[\left(\frac{k_0^2 n_1^2}{\beta^2} - 1\right)^{1/2} - \cos^{-1}\frac{\beta}{k_0 n_1}\right] - \tan^{-1}\left(\frac{\beta^2 - k_0^2 n_2^2}{k_0^2 n_1^2 - \beta^2}\right)^{1/2}$$

$$- \frac{\pi}{4} = m\pi. \qquad (23)$$

Similarly, for the step index profile of Fig. 1, $u_2 = -R_2 \ln R_2/R_1$, $u_3 = 0$, $h_{1^+,2} = 0$, $h_{3,4} = 0$, and the eigenvalue equation is[2]

$$R_2\beta\left[\left(\frac{k_0^2 n_2^2}{\beta^2} - 1\right)^{1/2} - \left(\frac{k_0^2 n_2^2}{\beta^2}\frac{R_1^2}{R_2^2} - 1\right)^{1/2} - \cos^{-1}\left(\frac{\beta}{k_0 n_2}\right)\right.$$

$$\left. + \cos^{-1}\left(\frac{\beta}{k_0 n_2}\frac{R_2}{R_1}\right)\right] - \tan^{-1}\left(\frac{\beta^2 - k_0^2 n_1^2\left(\frac{R_1}{R_2}\right)^2}{\left(\frac{R_1}{R_2}\right)^2 k_0^2 n_2^2 - \beta^2}\right)^{1/2}$$

$$- \tan^{-1}\left(\frac{\beta^2 - k_0^2 n_3^2}{k_0^2 n_2^2 - \beta^2}\right)^{1/2} = m\pi. \qquad (24)$$

For the diffused guide of Fig. 2, if the lateral diffusion results in an exponential-type decay of the form $n(\rho) = n_1 + (n_2 - n_1) \cdot \exp - [\zeta(\rho - R_2)/R_2]$ where ζ/R_2 is the decay rate of the index difference, the equivalent index profile is $n(u) = \exp \cdot [-\zeta \exp u/R_2 + \zeta + u/R_2]$. A closed form for $h_{3,4}$ is not known for such a profile. On the other hand, it is not difficult to generate approximations as is indicated in the next paragraph. Solutions of (23) and (24) can be obtained by graphical or numerical means.

The determination of α in closed form can be accomplished for index profiles exponential in the W plane. The results involve specification of $\sin (2 \tan^{-1} K_{4^-}/iK_{4^+})$, L, and $\exp (2ih_{4^+,5})$. These results are presented in Table I. For the diffused guide of Fig. 2 with exponential lateral diffusion, we approximate $n(u) \sim n_1 \exp u/R_2 + (n_2 - n_1) \exp - bu/R_2$, where b/R_2 is the
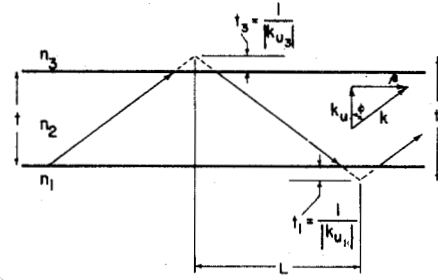

Fig. 9. The effective thickness t' and the effective longitudinal ray length L for a straight guide.

initial slope of $n(u)$ expressed in the previous paragraph; i.e., $b/R_2 = -[(1 - \zeta)/R_2] \exp \zeta$. An additional approximation for the diffused guide in Table I is made in the exponential term of α. We take

$$h_{4^+,6^-} \simeq 2[(\beta/k_0)^2 - n^2(u_5)]^{1/2}[u' - u_5] \qquad (25)$$

where u_5 is the point at which $n(u)$ is a minimum (Fig. 8), viz., $u_5 = (R_2/1 + b) \ln [b(n_2 - n_1)/n_1]$, and u' is the point at which $k_u(u)$ decreases by $1/\sqrt{2}$, viz., $[(\beta/k_0)^2 - n^2(u')]^{1/2} = (2)^{-1/2} \cdot [(\beta/k_0)^2 - n^2(u_5)]^{1/2}$.

Turning to a consideration of the dependence of β and α on the radius of curvature, we note that as the radius of curvature decreases, the index profile of the guide is skewed increasingly upward on the right. Fig. 10 illustrates this point. The figure shows a waveguide of constant thickness at different radii of curvature. Note that when $n_2(R_1/R_2) < n_3$, the behavior of the step waveguide of Fig. 1 is similar to that of the single boundary guide of Fig. 4 since the inner boundary lies in the evanescent region of the wave. Furthermore, there is a minimum radius of curvature R below which the single-boundary and two-boundary guides cease to carry any mode. From (23), setting $\tan^{-1}$ and m to zero and $\beta = k_0 n_2$,

$$R_{\min} = (\lambda_0/8)/[((n_1^2/n_2^2) - 1)^{1/2} - \cos^{-1}n_2/n_1] \qquad (26)$$

where λ_0 is the free-space wavelength. This same expression is obtained for the step index guide with n_1/n_2 replaced by n_2/n_3. When n_2 differs from n_1 by a small amount, $R_{\min}$ reduces to[3]

$$R_{\min} \simeq 0.1325 \lambda_0/[(n_1 - n_2)/n_1]^{3/2}. \qquad (27)$$

Using (26), $R_{\min} \simeq 0.45\lambda_0$ for $n_1/n_2 = 1.5$. Using (27), $R_{\min} \simeq 4200\lambda_0$ for $(n_1 - n_2)/n_1 = 10^{-3}$ and $R_{\min} \simeq 133\lambda_0$ for $(n_1 - n_2)/n_1 = 10^{-2}$.

When the radius of curvature is large compared to the wavelength, the value of β does not change radically from its value β_0 when the waveguide is straight. Using (24) to obtain a first-order expression for β in a step index guide, we find

$$\beta \simeq \beta_0 - \left(\frac{\partial [h_{1^+,4^-}]/\partial (1/R_2)}{-L}\right)\bigg|_{1/R_2=0} \cdot 1/R_2 = \beta_0(1 - t/2R_2)$$

$$(28)$$

---

[2]For small t/R_2, (24) reduces to $[k_0^2 n_2^2 - (\beta R_2/R_1)^2]^{1/2} t - \psi_1 - \psi_2 = m\pi$.

[3]Defining $\cos^{-1} n_2/n_1 = y$ and $[(n_1/n_2)^2 - 1]^{1/2} = \tan y$, for small y $\tan y - y \simeq 1/3y^3$.

TABLE I

	$\sin(2\tan^{-1}\frac{K_{4+}}{iK_{4-}})$	L	$\exp(2i\ h_{4+,6-})$
Single Boundary (Fig. 4)	$\dfrac{2(k_1^2-\beta^2)^{1/2}(\beta^2-k_2^2)^{1/2}}{k_1^2-k_2^2}$	$\dfrac{\beta}{(k_1^2-\beta^2)^{1/2}(\beta^2-k_2^2)^{1/2}} + R\cos^{-1}\dfrac{\beta}{k_1}$	$\exp\{2R(\beta^2-k_2^2)^{1/2}-2\beta R$ $\cdot\ln[\dfrac{\beta+(\beta^2-k_1^2)^{1/2}}{k_1}]\}$
Two Boundaries (Fig. 1)	$\dfrac{2(k_2^2-\beta^2)^{1/2}(\beta^2-k_3^2)^{1/2}}{k_2^2-k_3^2}$	$\dfrac{\beta}{[\beta^2-k_3^2(\frac{R_1}{R_2})^2]^{1/2}[k_2^2(\frac{R_1}{R_2})^2-\beta^2]^{1/2}}$ $+\dfrac{\beta}{(\beta^2-k_3^2)^{1/2}(k_2^2-\beta^2)^{1/2}}$ $+R_2[\cos^{-1}\dfrac{\beta}{k_2} - \cos^{-1}(\dfrac{\beta}{k_2}\cdot\dfrac{R_2}{R_1})]$	$\exp\{2R_2(\beta^2-k_1^2)^{1/2}-2\beta R_2$ $\cdot\ln[\dfrac{\beta+(\beta^2-k_3^2)^{1/2}}{k_3}]\}$
Diffused Guide (Fig. 2)	≈ 1	$\dfrac{R_2}{a}\cos^{-1}\dfrac{\beta}{k_2}(\dfrac{R_1}{R_2})^{a-2} + \dfrac{R_2}{b}\cos^{-1}\dfrac{\beta}{k_2}$ $+R_2[\cos^{-1}\dfrac{\beta}{k_2} - \cos^{-1}(\dfrac{\beta}{k_2}\dfrac{R_2}{R_1})]$	$\approx\exp\{-4[\beta^2-k^2(u_5)]^{1/2}(u'-u_5)\}$

Note: The attenuation along a bend is given by α as expressed in (20). The three parameters L, sin, and exp that are given in (20) are given for single-boundary, two-boundary, and diffused curved guides. For diffused guide parameters see the paragraph containing (25) and note that a and b are related to the initial slopes of the refractive index profile on the inner and outer boundary, respectively, of the guide. Note also that $k_j = k_0 n_j$.
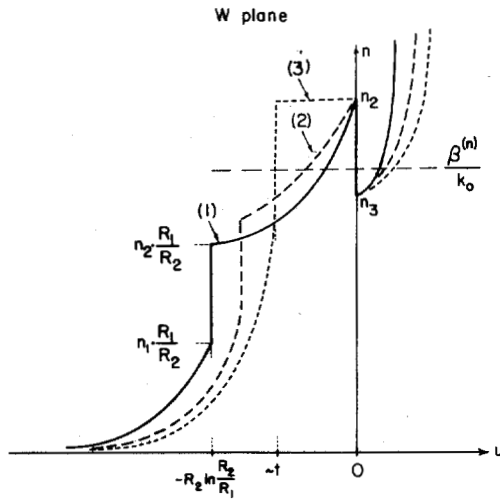

Fig. 10. Transformed index distribution of a step index guide of constant thickness at different radii of curvature. At small radius of curvature (1), i.e., when $R_1/R_2 < n_3/n_2$ the step index guide appears as a single-boundary guide. The dotted curve which corresponds to the largest radius of curvature should be labeled (3) and the dashed curve (2).

where $h_{1+,4-}$ is defined in (16), L is shown in (21), and t is the thickness of the guide $R_2 - R_1$. In (28) it is clear that a dramatic change in β occurs only when the radius of curvature approaches the guide thickness.

To consider the attenuation rate α expressed in (20), we note that the longitudinal ray path length has a simple geometric interpretation (Fig. 9) and is a number greater than the width of the equivalent guide. Unless $\exp(2ih_{4+,6-})$ is small, the attenuation is excessive. The exponential is small unless β approaches $k_0 n(u_5)$, where u_5 is the location of the index minimum (Fig. 8). For a prescribed αL we may specify a minimum β by solving equation (20) for β. Using the approximate expressions in Table I for a diffused waveguide and representing $n(u)$ near u_5 as $n(u_5) + (1/2)(\partial^2 n/\partial u^2)(u - u_5)^2$ we find

$$\beta_{min} \simeq k_0 n(u_5) + \ln{(\alpha L)^{-1}}/8[n(u_5)/(\partial^2 n/\partial u^2)_{u_5}]^{1/2}$$

where

$$n(u_5) = n_1 b\left(\frac{n_2}{n_1} - 1\right)^{1/b+1} + (n_2 - n_1)b\left(\frac{n_2}{n_1} - 1\right)^{b/b+1}$$

$$[n(u_5)/\partial^2 n/\partial u^2]^{1/2} = R_2\left[\frac{1 + b(n_2 - n_1)}{1 + b^3(n_2 - n_1)}\right]^{1/2} \qquad (29)$$

and b is related to the gradient of the lateral diffusion ζ/R_2 as discussed previous to (25). Using the value of L for a straight guide, (29) can provide a useful design relation for bends in diffused guides.

If we consider the attenuation rate of the step index guide (Fig. 1) for the situation in which $\beta = k_0 n_3(1 + \delta)$ differs by a small amount from the wavenumber of region 3, we find from Table I that the exponential term in α to first order in δ is

$$\alpha \propto \exp\left(-\frac{4\pi}{\lambda_0} R_2 n_3 \delta\right). \qquad (30)$$

This simple expression shows that unless the radius of curvature approaches the value $\lambda_0/4\pi n_3\delta \sim \lambda_0/4\pi(n_2 - n_3)$ the attenuation will be small. Even when the index difference is 10^{-3}, a radius of curvature of several hundreds λ_0 can be tolerated.

It should be emphasized that the two-boundary guide (Fig. 1) behaves like a one-boundary guide (Fig. 4) not only when $n_2(R_1/R_2) < n_3$ (as was noted before) but also when $n_2(R_1/R_2) \geqslant n_3$ and $\beta > n_2(R_1/R_2)$. In both cases, the expressions for β and α for the one-boundary guide should be used.

As a point of reference, in the limit of large radii of curvature $(R_2 \gg \lambda_0, t)$, the attenuation formula for a two-boundary guide (given in Table I) reduces to Marcuse's formula [2, eq. (32)] except for a factor of 2. This factor is the square of the transmission coefficient at the turning point and should be inserted in front of Marcuse's formula. The approximation for large radii can be shown easily by replacing the effective longitudinal ray length of the bend (L) by that of a straight guide (22) and by using $R_2 \gg t$.

IV. TRANSITION EFFECTS

The distortion in the index profile results in a displacement of the modes towards the outside of a bend and this effect results in transmission losses at the interfaces shown in Fig. 7. The WKB approximation of the spatial distribution of a mode in the region to the left of u_{6-} as obtained from (A6) is

$$
F(u) = \begin{cases}
(-1)^m \, [(|K_{4+}K_{4-}|)^{1/2}/|K_{4+} + K_{4-}|] \, (K_3/K)^{1/2} \exp i \int_{u_{4+}}^{u} k_u \, du, & u_{4+} < u < u_{6-} \\[3mm]
(K_3/K)^{1/2} \cos \left(\int_{u_{1+}}^{u} k_u \, du - \tan^{-1} \dfrac{K_{1-}}{iK_{1+}} \right), & u_{1+} < u < u_{4-} \\[3mm]
[(|K_{1+}K_{1-}|)^{1/2}/|K_{1+} + K_{1-}|] \, (K_3/K)^{1/2} \exp i \int_{u}^{u_{1-}} k_u \, du, & u < u_{1-}
\end{cases} \tag{31}
$$

where K is the same as in (18) for an arbitrary point u. This expression holds outside the turning points. The positions u_{1-}, u_{1+}, etc., are determined by requiring

$$
\left(\frac{\partial K/\partial u}{K} \frac{\pi}{k_u} \right)_{u_{i\pm}} = \epsilon \tag{32}
$$

where ϵ is a number much less than 1. Equation (32) is established by considering the second-order terms in the expansion of the system functions [11].[4]

Equation (31) indicates displacement of a mode because the argument of the cosine term contains an integral over $k_u = [k_0^2 n^2(u) - \beta^2]^{1/2}$ and the distortion in $n(u)$ results in a larger contribution from the right side of the guide than from the left. For the lowest order mode, the approximate peak occurs when the argument of the cosine is zero, i.e.,

$$
\int_{u_{1+}}^{u} k_u \, du = \tan^{-1} \frac{K_{1-}}{iK_{1+}}. \tag{33}
$$

Expressions for the integral in (33) may be obtained as in (23).

[4] The second-order term in the expansion of the system function is

$$
\frac{d}{du} \ln \frac{K(u_i)}{K(u)} \exp \left(i \int_{u}^{u_i} k_{u'} \, du' \right).
$$

and (24) using different representations in the regions $u_{1+} - u_2$, $u_2 - u_3$, $u_3 - u_{4-}$. The wave function within the guide region of a step index guide, for example, transformed back to the x, y plane is

$$
\begin{aligned}
F(\rho) = \left(\frac{k_2^2 - \beta^2}{k_2^2 \rho^2 / R_2^2 - \beta^2} \right)^{1/4} & \cos \left[(k_2^2 \rho^2 - \beta^2 R_2^2)^{1/2} \right. \\
& - \beta R_2 \cos^{-1} (\beta R_2/k_2 \rho) - (k_2^2 R_1^2 - \beta^2 R_2^2)^{1/2} \\
& \left. + \beta R_2 \cos^{-1} (\beta R_2/k_2 R_1) - \tan^{-1} \left(\frac{K_{1-}}{iK_{1+}} \right) \right]
\end{aligned} \tag{34}
$$

where $k_2 = k_0 n_2$ and

$$
\tan^{-1} \frac{K_{1-}}{iK_{1+}} = \tan^{-1} \left[\frac{\beta^2 - k_0^2 n_1^2 (R_1/R_2)^2}{k_2^2 (R_1/R_2)^2 - \beta^2} \right]^{1/2}. \tag{35}
$$

To provide a useful parameter we may determine the position of the peak ρ_0 of (34) in accordance with (33) to first order in $(\rho - R_1)/R_2$. The result is

$$
\rho_0 \simeq R_1 + \left(\tan^{-1} \frac{K_{1-}}{iK_{1+}} \right) \Big/ [k_0^2 n_2^2 - (\beta R_2/R_1)^2]^{1/2}. \tag{36}
$$

Approximating β as in (28), with $\beta_0 = (1 - \delta')k_0 n_2$ where δ' is presumed small, and retaining first-order terms in $1/R_2$, ρ_0 reduces to

$$
\rho_0 = \left(R_1 + \frac{t}{2} \right) + \frac{t}{2} \left\{ 1 - \frac{(2\delta')^{1/2} - 2t_3(\beta_0)/R_2}{[2\delta' + (t/R_2)^2]^{1/2}} \right\} \tag{37}
$$

where $t = R_2 - R_1$ and $t_3(\beta_0)$ is the evanescent decay distance into region 3 of a straight guide (Fig. 9). The displacement ρ_0 is sensitive to the radius of curvature as presented by (t/R_2) only when β_0 differs from $k_0 n_2$ by an amount of the order $1/2(t/R_2)^2$.

The power transmitted at the transition between guides of different curvature, as appear in Fig. 7, can be estimated by the overlap integral

$$
T^2 = 4 \frac{\left(\int F'F \, d\rho \right)^2 \Big/ \int F^2 \, d\rho \int F'^2 \, d\rho}{(1 + \beta'/\beta)^2} \tag{38}
$$

where F' and F are the wave functions of connecting guides and β' and β are the propagation constants. T^2 can be evaluated numerically for any given configuration using (31), or as a specific example, (34). The overlap integral depends on the direction of the displacement (36). To provide an estimate of the power transmitted at intersection (2) of Fig. 7, consider the approximation $F(\rho) \sim \cos a(\rho - \rho_0)$ and $F'(\rho) \sim \cos \cdot$

$a(\rho - \rho_0 + \Delta)$ where $a = \pi/2t$ and Δ represents the displacement between the two wave-function maxima in symmetric guides $(n_1 = n_3)$, viz., $\Delta = 2(\rho_0 - R_1) - t$. We obtain

$$T^2 = \left(1 - \frac{\pi^2 \Delta^2}{4t^2}\right)^2.$$ (39)

For small displacements the power loss is proportional to $(\Delta/t)^2$ and is a small percentage of the total. As Δ/t approaches unity there is, of course, substantial power loss. The overall power transmission of the structure shown in Fig. 7 may be approximated as a product of the form

$$T^2 = \left(1 - \frac{\pi^2 \Delta_1^2}{4t^2}\right)^2 \cdot (1 - \exp(-2\alpha R_2 \theta_1)) \cdot \left(1 - \frac{\pi^2 \Delta^2}{4t^2}\right)^2$$

$$\cdot (1 - \exp(-2\alpha R_2 \theta_2)) \cdot \left(1 - \frac{\pi^2 \Delta_1^2}{4t^2}\right)^2$$ (40)

where $\Delta_1 = \Delta/2$ is the displacement between guided-wave maxima at intersection (1) and θ_1 and θ_2 are the lengths of the arcs that make up a bend. Using (30) to approximate α and (37) to obtain Δ, (40) can provide a relatively simple approximation for the overall losses in a bend.

V. CONCLUSION

The method of conformal transformations has been shown to provide a useful qualitative as well as quantitative view of wave propagation in curved optical waveguides. The method requires no *a priori* limitations in radii of curvature or index differences. It has been shown how useful representations for the wave functions, eigenvalue equations, and attenuation constants can be obtained by analyzing equivalent structures in the transform plane. Using first-order approximations, simple expressions for the attenuation along a bend, the displacement of the wave from its position in a straight guide, the change in propagation constant due to bending of the guide, and the overall transmission loss in a practical bend have been presented.

APPENDIX

Solutions for the eigenfunctions and eigenvalue equations of continuously varying media may be obtained starting with solutions of a step discontinuous index profile containing constant index between steps. In such a profile, solutions to (3) or (5) are obtained by setting $\psi_j(u, v) = (1/K_j)(a_j^+ \exp ik_{u_j}u + a_j^- \exp -ik_{u_j}u) \exp ik_v v$ in layer j and matching boundary conditions at the interface between layers. The resulting equations in a_j^+ and a_j^- take the form

lines, respectively, are denoted $D_{1,2}$ and $D_{2,3}$. It is simple to show from (A1) that

$$D_{1,3} = D_{1,2}D_{2,3} - D'_{1,2}{}'D_{2,3}$$ (A2)

where the primes indicate

$$D'_{ij} = D_{ij}(k_{u_i}, \cdots, -k_{u_j}), \qquad 'D_{ij} = D_{ij}(-k_{u_i}, \cdots, k_{u_j}).$$ (A3)

Furthermore, it may be shown that (A2) can be generalized to any number layers in the form

$$D_{1,N} = D_{1,p}D_{p,N} - D'_{1,p}{}'D_{p,N}$$ (A4)

where p is any layer between 1 and N.

The complex propagation constant for a guided wave is the value of k_v for which the determinant in (A1) is zero. The eigenvalue equation is thus

$$(D_{1,N})_{k_v = \beta + i\alpha} = 0.$$ (A5)

Furthermore, it may be shown that the eigenfunction can be expressed

$$F(u) = A\left[\frac{D_{1,p}}{2K_1 \cdots 2K_p} \exp(-ik_{u_p}u) - \frac{D'_{1,p}}{2K_1 \cdots 2K_p}\right.$$

$$\left. \cdot \exp(ik_{u_p}u)\right], \qquad u_{p-1} < u < u_p$$ (A6)

where p refers to any layer in which (A6) is evaluated and A is a constant.

If the number of layers is permitted to become infinite and $n(u)$ becomes continuous, it is possible to represent the system functions in a series of the kind first described by Bremmer [10] and presented by Harris [11]. The first terms of the series are the WKB forms

$$D_{r,q}/(2K_r) \cdots (2K_{q-1}) \simeq (K_q/K_r)^{1/2} \exp\left[-i\int_{u_r}^{u_{q-1}} k_u \, du\right.$$

$$\left. + i(k_{u_q}u_{q-1} - k_{u_r}u_r)\right]$$

$$'D_{r,q}/(2K_r) \cdots (2K_{q-1}) \simeq -(K_q/K_r)^{1/2} \exp\left[i\int_{u_r}^{u_{q-1}} k_u \, du\right.$$

$$\left. - i(k_{u_q}u_{q-1} - k_{u_r}u_r)\right]$$

$$D'_{r,q} = {}'D_{r,q} = 0.$$ (A7)

$$\begin{bmatrix} -K_1 \exp(-ik_{u_1}u_1) & -K_2 \exp(ik_{u_2}u_1) & K_2 \exp(-ik_{u_2}u_1) & 0 \\ \exp(-ik_{u_1}u_1) & -\exp(ik_{u_2}u_1) & -\exp(-ik_{u_2}u_1) & 0 \\ 0 & K_2 \exp(ik_{u_2}u_2) & -K_2 \exp(-ik_{u_2}u_2) & -K_3 \exp(ik_{u_3}u_2) \\ 0 & \exp(ik_{u_2}u_2) & -\exp(-ik_{u_2}u_2) & -\exp(ik_{u_3}u_2) \end{bmatrix} \begin{bmatrix} a_1^- \\ a_2^+ \\ a_2^- \\ a_3^+ \end{bmatrix} = 0$$ (A1)

where the k_u and K's are defined, respectively, in (15) and (18), the subscript refers to the layer, and u_1 and u_2 are two interfaces for a three-region problem.

The determinant of the matrix in (A1) is denoted $D_{1,3}$, while the determinants of the matrix within the dotted and dashed

Near a turning point (A7) fails and we have

$$D_{r,q} \simeq (2K_r) \cdots (2K_{q-1})\left(\frac{K_r + K_q}{2K_q}\right) \exp i(k_{u_q}u_{q-1} - k_{u_r}u_r).$$ (A8)

The primes of (A8) are obtained as in (A3). The subscripts in (A7) and (A8) refer to sublayers as indicated in Fig. 8 and are described more fully in the next paragraph.

To express (A5) or (A6) for continuously varying media to the approximation (A7) and (A8) we employ (A4) sequentially stopping at each turning point (u_1, u_4, and u_6 of Fig. 8) and write, for example,

$$D_{1,6} = D_{1,1}\{[D_{1^-,1^+}D_{1^+,4^-}D_{4^-,4^+} + D'_{1^-,1^+}{}'D'_{1^+,4^-}{}'D_{4^-,4^+}]$$

$$\cdot D_{4^+,6^-}D_{6^-,6^+} + [D_{1^-,1^+}D_{1^+,4^-}D'_{4^-,4^+} + D'_{1^-,1^+}{}'D'_{1^+,4^-}{}'D'_{4^-,4^+}]$$

$$\cdot {}'D'_{4^+,6^-}{}'D_{6^-,6^+}\}D_{6^+,6}. \tag{A9}$$

The zero functions of the third equation in (A7) have been incorporated in (A9). Subscript 1 refers to the point u_1 located to the left of u_{1^-} as indicated in Fig. 8. Similarly, 6 refers to u_6 located to the right of u_{6^+}. Using the first equation in (A7) to describe the way the subscripts are used, we have

$$\frac{D_{1,1^-}}{2K_{u_1} \cdots 2K_{u_1}} = (K_{u_{1^-}}/K_{u_1})^{1/2} \exp\left\{-i\int_{u_1}^{u_{1^-}} k_u\, du\right.$$

$$\left. + i[k_u(u_{1^-})u_{1^-} - k_u(u_1)u_1]\right\}. \tag{A10}$$

Note that to employ (A7) and (A8) conveniently, (A5) can also be written $D_{1,N}/2K_1 \cdots 2K_N = 0$.

The equation for β is obtained by neglecting the region to the right of u_{4^+} and can be expressed as

$$(D_{1,4^+}/2K_{u_1} \cdots 2K_{u_{4^+}})_{k_v=\beta} = 0. \tag{A11}$$

The equation for $i\alpha = (k_v - \beta)$ is obtained by setting $D_{1,6}$ to zero, expressing

$$(D_{1,4^+}/2K_{u_1} \cdots 2K_{u_{4^+}})_{k_v \simeq \beta} \simeq \left(\frac{\partial}{\partial k_v} D_{1,4^+}/2K_{u_1} \cdots 2K_{u_{4^+}}\right)_\beta$$

$$\cdot (k_v - \beta)$$

and using (A4) with p at u_{4^+}. The result is

$$i\alpha = \left[\frac{(D'_{1,4^+}/2K_{u_1} \cdots 2K_{u_{4^+}})D_{4^+,6}}{\left(\frac{\partial}{\partial k_v} D_{1,4^+}/2K_{u_1} \cdots 2K_{u_{4^+}}\right){}'D_{4^+,6}}\right]_{k_v=\beta}. \tag{A12}$$

In the text $K_j^\pm$ is used instead of $K_{u_j^\pm}$. Finally, the wave function is expressed using (A6) treating u_p as an arbitrary point u.

REFERENCES

[1] a) E. A. Marcatili, "Bends in optical dielectric guides," *Bell Syst. Tech. J.*, vol. 48, pp. 2103–2132, Sept. 1969.
b) D. Marcuse, "Bending losses of the asymmetric slab waveguide," *Bell Syst. Tech. J.*, vol. 50, pp. 2551–2563, Oct. 1971.
c) L. Lewin, "Radiation from curved dielectric slabs and fibers," *IEEE Trans. Microwave Theory Tech.*, vol. MTT-22, pp. 718–727, July 1974.
[2] R. S. Elliott, "Azimuthal surface waves on circular cylinders," *J. Appl. Phys.*, vol. 26, pp. 368–376, Apr. 1955.
[3] H. F. Taylor, "Power loss at directional change in dielectric waveguides," *Appl. Opt.*, vol. 13, pp. 646–647, Mar. 1974.
[4] F. E. Borginis and C. H. Papas, "Electromagnetic waveguides and resonators," in *Handbuch der Physik*, vol. 16, S. Flügge, Ed., pp. 358–364.
[5] W. E. Martin, "Waveguide electro-optic modulation in II-VI compounds," *J. Appl. Phys.*, vol. 44, pp. 3703–3707, Sept. 1973.
[6] a) E. A. Marcatili, "Dielectric rectangular waveguide and directional coupler for integrated optics," *Bell Syst. Tech. J.*, vol. 48, pp. 2071–2102, Sept. 1969.
b) J. E. Goel, "A circular-harmonic computer analysis of rectangular dielectric waveguides," *Bell Syst. Tech. J.*, vol. 48, pp. 2133–2160, Sept. 1969.
[7] R. K. Winn and J. H. Harris, "Coupling from multimode to single-mode linear waveguides using horn-shaped structures," *IEEE Trans. Microwave Theory Tech.*, vol. MTT-23, pp. 93–97, Jan. 1975.
[8] a) D. Marcuse, "Mode conversion caused by slab imperfections of a dielectric slab waveguide," *Bell Syst. Tech. J.*, vol. 48, pp. 3187–3215, Dec. 1969.
b) J. H. Harris, R. K. Winn, and D. Dalgoutte, "Theory and design of periodic coupler," *Appl. Opt.*, vol. 11, pp. 2234–2241, Oct. 1972.
[9] a) L. V. Iogansen, "Theory of resonant electromagnetic systems with total internal reflection III," *Sov. Phys.–Tech. Phys.*, vol. 11, pp. 1529–1534, May 1967.
b) J. H. Harris, R. Shubert, and J. N. Polky, "Beam coupling to films," *J. Opt. Soc. Amer.*, vol. 60, pp. 1007–1016, Aug. 1970.
[10] H. Bremmer, "The WKB approximation as the first term of a geometrical optical series," *Commun. Pure Appl. Math.*, vol. 4, pp. 105–115, June 1951.
[11] J. H. Harris, "Analysis techniques for multilayer structures," *IEEE Trans. Microwave Theory Tech.*, vol. MTT-23, submitted.
[12] Lord Rayleigh, "The problem of the whispering gallery," in *Scientific Papers*, vol. 5. London: Cambridge, 1912, pp. 617–620.
[13] The following references contain material related to this article.
a) S. J. Maurer and L. B. Felsen, "Ray methods for trapped and slightly leaky modes in multilayered or multiwave regions," *IEEE Trans. Microwave Theory Tech.*, vol. MTT-18, pp. 584–595, Sept. 1970.
b) D. C. Chang and F. S. Barnes, "Reduction of radiation loss in a curved dielectric slab waveguide," Electromagnetic Lab., Dep. Elec. Eng., Univ. Colorado, Boulder, Sci. Rep. 2, July 1973.
c) D. Marcuse, "Bent optical waveguide with lossy jacket," *Bell Syst. Tech. J.*, vol. 53, pp. 1079–1101, July 1973.
d) S. Sheem and J. R. Whinnery, "Guiding by single curved boundaries in integrated optics," *Wave Electron.*, vol. 1, to be published.
e) ——, "Modes of a curved surface waveguide for integrated optics," *Wave Electron.*, vol. 1, to be published.